Colloid & Polymer Science Colloid Polym Sci 272:846–854(1994)

Self diffusion and viscoelasticity of elongated micelles from cetyltrimethyl-ammonium bromide in aqueous sodium salicylate solution. II. Temperature effect

N. Nemoto and M. Kuwahara

Institute for Chemical Research, Kyoto University, Japan

Abstract: Forced Rayleigh scattering and dynamic viscoelastic experiments are performed to study slow global motions of networks formed by elongated micelles from cetyltrimethylammonium bromide (CTAB) in aqueous sodium salicylate (NaSal) solutions at six temperatures T from 25° to 60 °C. The CTAB concentration C_D of the solutions is fixed at $C_D = 0.01$ M and a ratio of salt concentration C_s to C_D is varied from 1 to 41. The self-diffusion coefficient D of the dye-labeled cetyldimethylamine incorporated in the micelles shows a complicated C_s/C_D dependence with a maximum that is followed by a minimum at lower temperatures, but these two extremes gradually disappear with increasing T. The C_s/C_D dependencies of both the steady-state viscosity η and the terminal relaxation time τ are found consistent with the diffusion behavior. The D of all solutions tested monotonically increases with T, but shows different functional dependence on T as C_s/C_D varies. The applicability of the theory of Brownian motion of a rigid rod in the semidilute regime is examined using D and τ values.

Key words: CTAB:NaSal micelles – self diffusion coefficient – dynamic viscoelasticity – forced Rayleigh scattering – temperature effect

Introduction

In recent years, elongated micelles from a combination of surfactant and suitable salt in water have drawn considerable interest of experimentalists and theoreticians for their unique viscoelastic properties [1–22]. Elongated micelles of alkyltrimethylammonium and alkylpyridinum salts are typical examples, and their characteristics and network properties are extensively studied using other techniques such as electron microscopy [23–25], NMR [26–30], neutron scattering [31, 32], static and dynamic light scattering (DLS) [33–45], flow and electric birefringence [46–48], and fluorescence recovery after photo bleaching and forced Rayleigh scattering [49, 50].

In a series of papers [50–52], we have also studied dynamic aspects of networks formed by elongated micelles of cetyltrimethylammonium bromide (CTAB) in aqueous sodium salicylate (NaSal) solution with three methods of DLS, FRS, and dynamic viscoelasticity (DVE) over a wide range of the surfactant concentration C_D and of the salt concentration C_s. In these studies, we took into account the fact that fast local motions of the network are effectively proved by DLS, while slow global motions are proved by FRS and DVE. Noticeable findings from these studies along with the DVE work by Shikata et al. [6] are 1) the first cumulant Γ_e showed a complicated dependence, not only on C_D, but also on C_s/C_D at low C_D. However, the reduced plot of Γ_e/q^2D_c vs. $q\xi_H$ gave one master curve for all Γ_e data where D_c and ξ_H are the cooperative diffusion coefficient and the hydrodynamic correlation length, respectively and q the scattering vector; 2) at higher C_D, DLS detected the fast diffusive mode and the slow relaxation mode. The D_c estimated from q-independent Γ_e/q^2 for the fast mode

followed the power law of $D_c \propto C_D^{0.45}$ in agreement with the prediction for a rod in the semidilute regime; 3) very complicated C_D and C_s/C_D dependencies are found for the self-diffusion coefficient D of dye-labeled cetyldimethylamine incorporated in the micelles as well as the mechanical relaxation time τ obtained from a fit of DVE data to a Maxwell type of model with the single relaxation time. Each of the data could be reduced to one master curve by plotting either D or τ against the concentration C_s^* of free salicylate ion Sal^- in water. The above results look to demonstrate that the specific interaction between CTA^+ cation and Sal^- anion plays an important role for dynamical behavior of this micelle system.

In this work, the effect of temperature on the dynamics of CTAB:NaSal micelle network is explored for the samples with a constant value of $C_D = 0.01$ M and varying C_s/C_D from 1 to 41 using the FRS and the DVE techniques. The diffusion and the viscoelastic behaviors varied in a very consistent manner as temperature increased, so that the maximum and the minimum observed in the plots of D and τ against C_s/C_D at $T = 25\,^\circ$C might gradually disappear with increasing T. The results clearly indicate that the same dynamical mechanism is operating for diffusion and mechanical relaxation of this CTAB:NaSal micelle system.

Experimental

Materials

Twice-recrystallized cetyltrimethylammonium bromide (CTAB) (Nacarai Tesque) and special-grade sodium salicylate (NaSal) (Nacarai Tesque) were used as cationic surfactant and salt samples in this study. Dust-free purified water (resistance $> 16.5\ M\Omega$) was used as solvent. Cetyldimethylamine (CDA) labeled with a photochromic dye of 4-(bromomethyl) azobenzene was used as a probe molecule for measurements of the self diffusion coefficient D of the micelles with the forced Rayleigh scattering method. Aqueous solutions of the CTAB:NaSal micelles were prepared by mixing prescribed amounts of aqueous solutions of CTAB containing labeled CDA and of NaSal solutions and by equilibriating at room temperature for at least 2 days. The surfactant concentration C_D of seven solutions tested was fixed at 0.01 M and ratios of the salt concentration C_s to C_D were 1, 1.2, 2, 4, 10, 20, and 41.

Methods

Forced Rayleigh scattering experiments were performed with an instrument described elsewhere [53, 54]. Monochromatic light of an Ar ion laser ($\lambda = 488$ nm) with an output power of 400 mW and that of a He-Ne laser ($\lambda = 633$ nm) with an output power of 1 mW were used as a writing and a reading coherent beam, respectively. Acquisition and analysis of time profiles of light intensity data diffracted from the solutions were handled with a home-made processor. FRS measurements were made at six temperatures of 25°, 33°, 40°, 50°, 55°, and 60 °C.

Dynamic viscoelastic measurements were made with a Couette-type rheometer (Rheometrix, Fluid Spectrometer RFSII). The storage and loss shear moduli, $G'(\omega)$ and $G''(\omega)$, were measured over the angular frequency range from 1×10^{-2} to $6 \times 10\ \text{rads}^{-1}$ at four temperatures of 25°, 33°, 40°, and 50 °C. Reliable G^* data were not obtained at 60 °C.

Results and discussion

Forced Rayleigh scattering (FRS)

An example of time profiles of $I_d(t)$ diffracted from aqueous solutions of elongated CTAB:NaSal micelles is shown in Fig. 1 for the solution with $C_s/C_D = 2$ at 25 °C. It is seen from the figure that $I_d(t)$ does not monotonically decrease with elapse of time but takes a maximum immediately after the sample is irradiated by the intense laser beam of 400 mW. The initial rise in the $I_d(t)$ curve was mostly finished within a time period less than 0.05 s, and might be attributed to a rearrangement or reorientation process of the photochromic dye of the methylazobenzene residue in the tightly packed micelle which undergoes cis-trans conformational transition by irradiation of light. Data fitting with a single exponential type of decay function, Eq. (1), was, therefore, made using data points which decrease with t after a maximum was attained, for example,

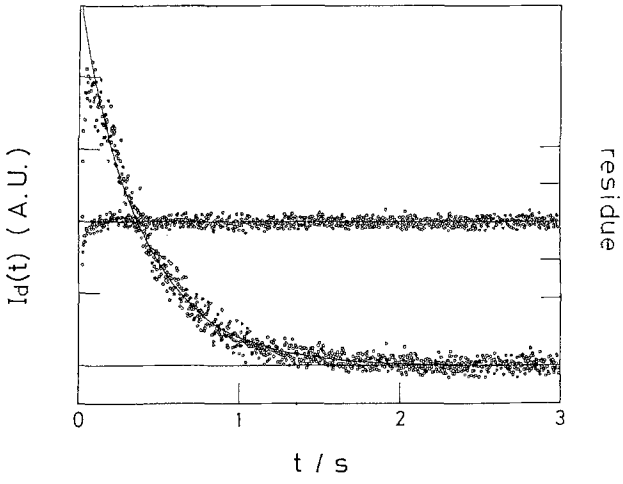

Fig. 1. A time profile of $I_d(t)$ diffracted from the CTAB:NaSal micelles in aqueous solution with C_D = 0.01 M and $C_s/C_D = 2$ at 25 °C. Residues indicate that the decay is a single-exponential type for t > 0.1 s

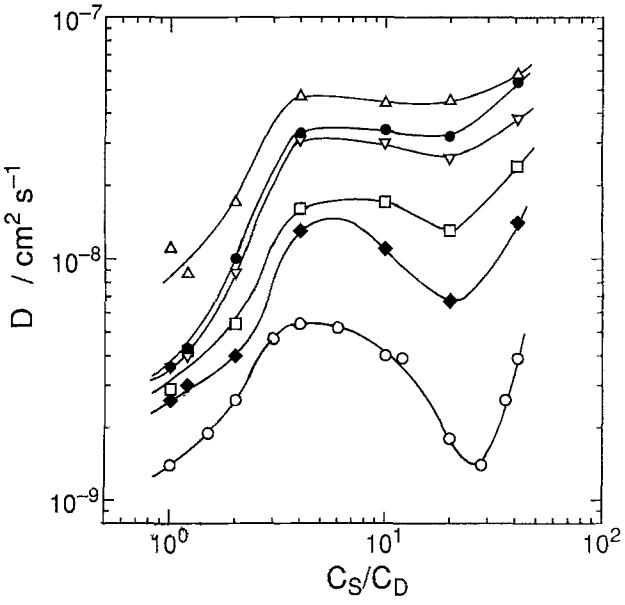

Fig. 2. The self-diffusion coefficient D of the CTAB:NaSal micelles in aqueous solution plotted against C_s/C_D at six temperatures. Symbols for T are (○) 25, (◆) 33, (□) 40, (▽) 50, (●) 55, and (△) 60 °C. Solid curves are empirically drawn as a guide for the eye

data points for $t > 0.1$ s in the analysis of the $I_d(t)$ curve shown in the figure.

$$I_d(t) = \{A \exp(-\Gamma t) + B_1\}^2 + B_2^2 \quad (1)$$

$$\Gamma = Dq^2 \quad (2)$$

Here, A is the amplitude and B_1 and B_2 are contributions from coherent and incoherent background optical field, respectively, and q is the scattering vector to be calculated from the grating spacing p as $q = 2\pi/p$. The fitted curve, given as the solid curve in the figure, fairly reproduces the time dependence of $I_d(t)$ with small random values of residuals shown in the same figure. The Γ/q^2 values obtained at $p = 2$ and 4 μm were in good agreement with each other to an accuracy of 10% for all solutions and a straight line connecting two Γ values of each solution in a Γ vs q^2 plot was found to cross the origin within experimental uncertainty. Thus, the effect of the finite lifetime of the dye on Γ may be negligible and the decay process of $I_d(t)$ is not anomalous diffusion like a Levy process as is found for the CTAB:KBr micelles under a limited range of C_D and C_s/C_D by Ott et al. [55], but may be considered as normal diffusion, although the q range covered by our FRS experiment is pretty narrow. The diffusion coefficient D was then estimated as the average of two Γ/q^2 values. As was reported in an earlier paper [50], the same D value was obtained for solutions with different values of a relative fraction f of labeled-CDA to total surfactant concentration C_D at fixed C_D and C_s/C_D, as far as f was kept less than 0.06. This may indicate that probe molecules are incorporated in micelles and do not perturb the micelle structure for $f < 0.06$. It is noteworthy that the CTAB:NaSal micelles break into pieces, i.e., a very short one and a spherical one at around 80 °C. Eventually the diffracted intensity $I_d(t)$ did not monotonically decay but bounced up and down several times at intermediate time at 70 °C, which made it impossible to determine Γ by the fitting procedure with Eq (1).

The diffusion coefficient D of the solutions measured at six temperatures is plotted against C_s/C_D in Fig. 2. The maximum and the minimum in D with increasing C_s/C_D clearly observed at 25 °C are the characteristic features of this micellar system. The unique C_s/C_D dependence of D appears to persist at elevated temperatures of 33° and 40 °C, while the height and the depth gradually become smaller. Above 50 °C, D rapidly increases at low C_s/C_D by nearly an order of magnitude, takes an almost constant value at intermediate C_s/C_D, and once again increases at the large C_s/C_D end. Stated another way, a rise of

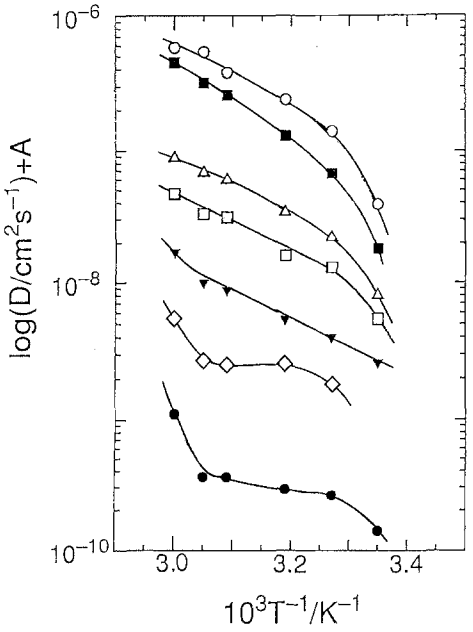

Fig. 3. Temperature dependence of D of the CTAB:NaSal micelles in aqueous solution at seven C_s/C_D values. The respective data are vertically shifted by a factor A in the logarithmic scale for clarity of the figure. Symbols for C_s/C_D and A are (●) 1, −1, (◇) 1.2, −0.2, (▼) 2, 0, (□) 4, 0, (△) 10, 0.3, (■) 20, 1, and (○) 40, 1, respectively

temperature induces the disappearance of the minimum at large C_s/C_D.

At constant C_s/C_D, D of the solutions monotonically increases with an increase in T. In looking into the T dependence of D of each solution more closely by replotting D against T semilogarithmically, we find different types of functional dependence of D on T as C_s/C_D varies. As is shown in Fig. 3 where solid curves are empirically drawn as a guide for the eye, D at $C_s/C_D = 1$ and 1.2 appears to increase with T in two steps. At $C_s/C_D = 2$, the functional form becomes close to the Arrhenius type. With further increase in C_s/C_D, the plot is fairly represented by smooth curves with steeper curvature as T increases. This kind of variation in T dependence of D with varying C_s/C_D has not been reported hitherto as far as the authors are aware of, and may be characteristic of this CTAB:NaSal micelle system.

Dynamic viscoelasticity (DVE)

Figure 4 gives angular frequency ω dependence of the storage and the loss shear moduli, $G'(\omega)$ and $G''(\omega)$, of six CTAB:NaSal micelle solutions with a fixed value of $C_D = 0.01$ M and varying C_s/C_D from 1 to 41 at $T = 40$ °C. The characteristic feature of the terminal zone, $G'(\omega) \propto \omega^2$, and $G''(\omega) \propto \omega$, are clearly observed for all data. Both G' and G'', first make a shift to the right

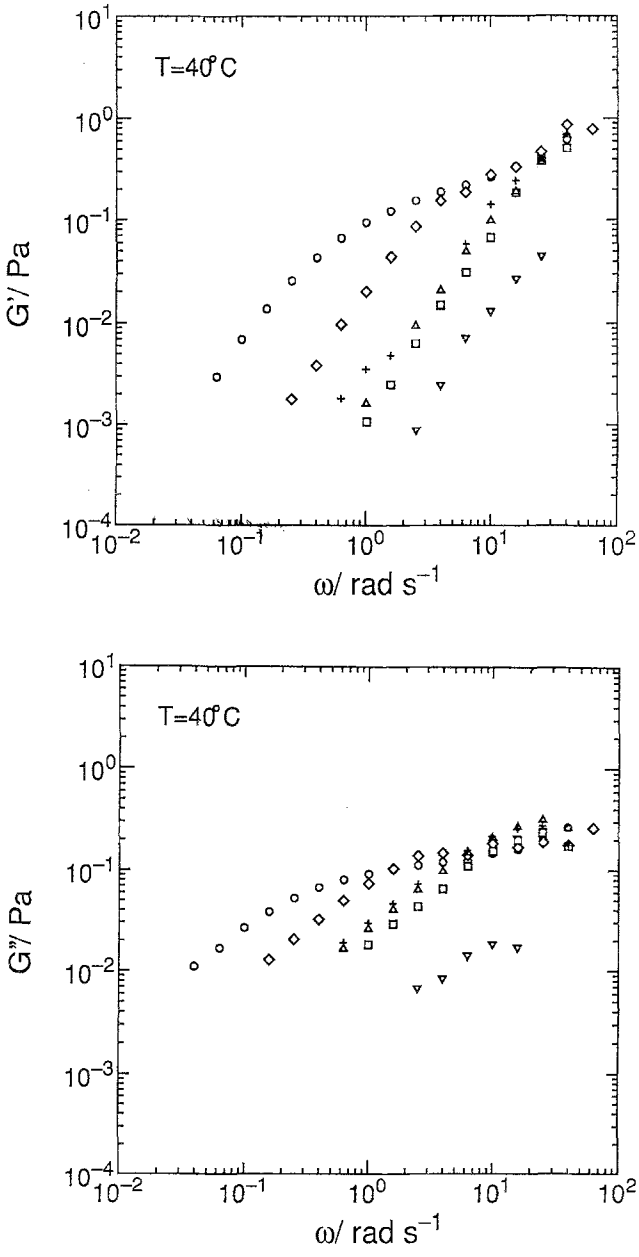

Fig. 4. The storage and loss shear moduli, $G'(\omega)$ and $G''(\omega)$, of the CTAB:NaSal micelles in aqueous solution with varying C_s/C_D at 40 °C plotted against the angular frequency ω. Symbols for C_s/C_D are (○) 1, (◇) 2, (□) 4, (△) 10, (+) 20, (▽) 41

Table 1. Values of the self-diffusion coefficient D, the shear viscosity η, the steady-state compliance J_e and the terminal relaxation time τ as $\tau = \eta J_e$ of the CTAB:NaSal micelles in aqueous solution

T°C	$D/10^{-9}$ cm^2 s^{-1}						$\eta/10^{-2}$Pas				J_e/Pa^{-1}				τ/s			
C_s/C_D	25	33	40	50	55	60	25	33	40	50	25	33	40	50	25	33	40	50
1	1.4	2.6	2.9	3.6	3.6	11	–	180	26	1.5	–	9.2	7.7	7.3	100	17	2	0.11
1.2	–	3.0	4.2	4.0	4.3	8.7	–	–	–	–	–	–	–	–	–	–	–	–
2	2.6	4.0	5.4	8.8	10	17	100	25	8	1.8	4.1	4.0	4.4	3.7	4.1	1.0	0.35	0.067
4	5.4	13	16	31	33	47	14	2.2	1.8	0.76	3.3	3.2	3.3	5.0	0.46	0.07	0.059	0.038
10	4.0	11	17	30	34	44	87	18	3.7	0.45	1.9	1.9	2.2	8.3	1.7	0.34	0.08	0.037
20	1.8	6.7	13	26	32	45	19	8.5	3	0.8	4.8	2.5	2.5	10	0.91	0.21	0.075	0.08
41	3.9	14	24	38	54	58	0.8	0.55	0.25	0.13	5.0	6.6	25	120	0.04	0.036	0.063	0.16

a. From ref. [50].

along the frequency axis with increasing C_s/C_D which is followed by a shift to the left in the range of C_s/C_D from 4 to 20, and finally to the right at $C_s/C_D = 41$. The behavior is quite similar to that observed at 25 °C [50]. However, the plateau in G' and the maximum in G'' which are clearly observed for the data at 25 °C cannot be seen in the data at 40 °C, even though they cross each other at intermediate ω. This implies that the average micelle length at $C_D = 0.01$ M and $T = 40$ °C may not be long enough to form a tight entanglement network by overlapping of elongated micelles. A rise in G' and G'' at the high ω side indicates the presence of an additional relaxation mechanism, probably due to the intramolecular motion of micelles. Therefore data fitting using a Maxwell type of model with the single relaxation time τ seems inapplicable. Instead, the steady viscosity η and the steady-state compliance J_e were estimated from values of G' and G'' in the terminal zone with Eq. (3).

$$G'(\omega) = \eta^2 J_e \omega^2, \quad G''(\omega) = \eta\omega \,. \tag{3}$$

The relaxation time τ was calculated as $\tau = \eta J_e$. Values of η, J_e, and τ thus estimated are listed with D in Table 1.

In order to show changes in ω dependence of G' and G'' with T, G', and G'' of the solution of $C_s/C_D = 2$ at four temperatures are plotted against ωa_T in Fig. 5 where the data above 50 °C are not shown because of poor reproducibility. Here, a_T is the correction factor which takes into account the decrease in the local friction factor with T and may be calculated as $a_T = \eta_{s,T} T_0/\eta_{s,T_0} T$ [56], where $\eta_{s,T}$ is solvent viscosity at T and the reference temperature T_0 is taken as 25 °C. G' and G'' both shift to the right along the frequency axis with increasing T, so that the plateau in G' and the maximum in G'' tend to disappear. Such a monotonic T dependence is consistent with the diffusion behavior. Interestingly, the data at different T appear to be superposed to one another at high ω by virture of the shift factor a_T. In an earlier study [51], we estimated the first cumulant Γ_e from dynamic light-scattering experiments on the same samples at 25°, 33° and 40 °C for a study of the intramolecular motions of network strands of elongated micelles in the semidilute regime. The reduced plot of $\Gamma_e/q^2 D_c$ against $q\xi_H$ gave one master curve with the slope of about unity for $q\xi_H \gg 1$. Here, D_c is the cooperative diffusion coefficient as $D_c = (\Gamma_e/q^2)_{q\to 0}$ and ξ_H is the hydrodynamic correlation length as $\xi_H = k_B T/(6\pi\eta_s D_c)$. Thus, DLS and DVE prove the same molecular motion which might be assigned as bending motions of the elongated micelles.

Figure 6 shows the dependence of τ on C_s/C_D at four temperatures. At 25° and 33 °C, τ first decreases rapidly with increasing C_s/C_D and takes a minimum and consecutively a maximum in correspondence to the diffusion behavior in Fig. 2. The value of $C_s/C_D = 4$ at the minimum of τ agrees with that at the maximum of D, but the maximum of τ occurs at $C_s/C_D = 10$ smaller than 20 for the minimum of D. At 40 °C a rapid decrease in τ at low C_s/C_D persists, and a small minimum and a maximum are observed at $C_s/C_D = 4$ and 20, respectively. This behavior is consistent with the diffusion behavior at the same temperature over the entire C_s/C_D range investigated. Consistency between τ and D holds also for

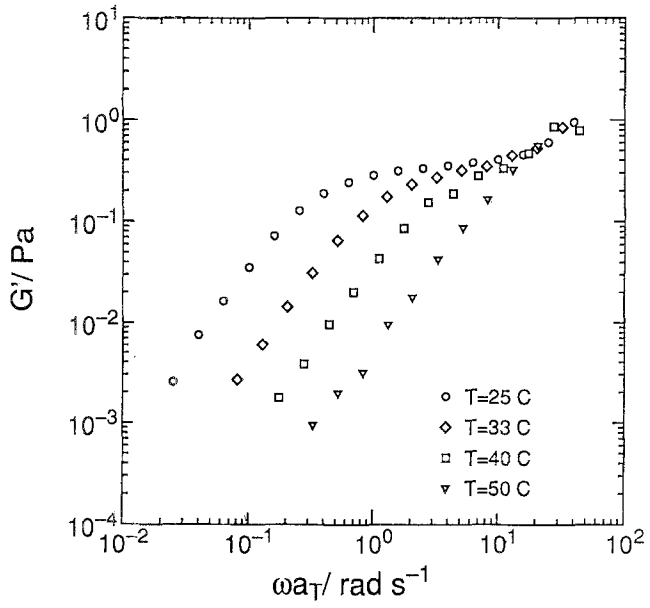

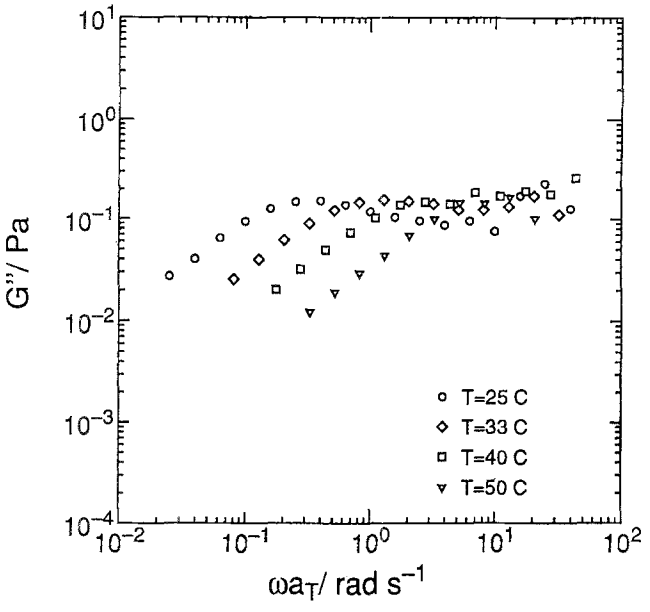

Fig. 5. The G′ (ω) and G″ (ω) of the CTAB:NaSal micelles in aqueous solution with $C_s/C_D = 2$ plotted against ωa_T at four temperatures. Symbols for T are (○) 25°, (◇) 33°, (□) 40°, and (▽) 50 °C

the data at 50 °C except an increase in τ at $C_s/C_D = 41$ which was brought by a large increase in J_e. Such inconsistency is not present for the viscosity data and D data. By taking into account the earlier results that D and τ behave consistently concerning their dependence on the surfactant concentration [50], we may conclude that FRS

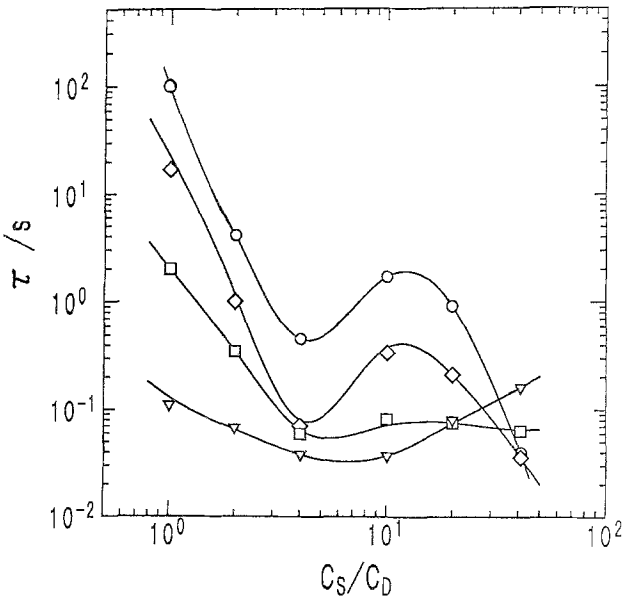

Fig. 6. The terminal relaxation time $\tau = \eta J_e$ plotted against C_s/C_D at four temperatures. Symbols for T are the same as in Fig. 5. Solid curves are empirically drawn as a guide for the eye

and DVE techniques effectively detect the same slow global molecular motion of the CTAB: NaSal micelles in solution.

Brownian motion of a rod in the semidilute regime

We had better to start from qualitative discussion about effects of T and C_s/C_D on the solution structure as well as average length and flexibility of the CTAB:NaSal micelles. The micelle is stabilized by forming a 1:1 complex of a CTA^+ cation and a Sal^- anion in addition to the intermolecular hydrophobic and electrostatic forces between surfactants. Thus, the salt is considered to affect the micelle structure in two different ways. At low salt concentration just above $C_s/C_D = 1$, excess Sal^- ions incorporated in the micelle deteriorate the micelle structure. With increasing C_s the NaSal salt in water can also act as conventional salt like NaBr. The former effect is very effective at low C_s and may give rise to shortening of the equilibrium micelle length and to an increase in flexibility, whereas the latter as the salt-out effect may lengthen and stiffen the micelle at higher C_s. Competition of these two

effects may induce the maximum in D and τ^{-1} with increasing salt concentration as is observed at 25° and 33 °C. This speculation is supported by a result of electrophoretic light scattering experiments that the CTAB:NaSal micelle changes the sign of electric charge with increasing C_s at 25 °C from a positive to negative one at around $C_s/C_D = 6$ [57]. Similar behavior has already been reported for the CTASal/NaSal system by Olsson et al. [29] and Imae [42]. The micelle is increasingly more negatively charged at high salt concentration, not only by adsorption of Sal^- ions on the micelle surface, but also by their penetration into the interior of the micelle. Also, there occurs a rapid exchanging reaction between Sal^- ions incorporated in the micelles and those being free in water under thermodynamical equilibrium. Those disturbances by large amounts of excess Sal^- ions on the micelle structure finally overcomes the salt-out effect, which may lead to an increase in D and an decrease in τ once again, possibly due to breaking into shorter micelles.

A rise of temperature seems to simply deteriorate or loosen the micelle structure formed by the intermolecular forces. Therefore, D should monotonically increase with T at any C_s/C_D. In the low C_s/C_D range where Sal^- ions mainly disturbs the micelle structure, D should increase more sharply with C_s at elevated temperature, and in the region where the salt-out effect becomes dominant, the decrease in D after the maximum must be small. Those conjectures qualitatively explain the unique diffusion as well as viscoelastic behaviors observed for the CTAB:NaSal micelle system.

In an earlier paper [50], we discussed applicability of the theory of Brownian motion of a rigid rod in the semidilute regime for the dynamics of the CTAB:NaSal micelle system. The micelle is certainly not a rigid rod as is manifested by the presence of the mechanical relaxation at the high frequency side, but may be better represented by the wormlike chain model. Dynamic viscoelastic studies on dilute solutions of stiff polymer molecules [58–62] show that there are two relaxation modes, one being a Zimm-like mode related to bending motions of polymer chains and the other the single relaxation mode related to the end-over-end rotation of the whole chain. We expect that these modes are also observable in the semidilute regime in a well separated time scale. Extending this idea to the CTAB:NaSal micelles overlapped in aqueous solution, we assume that the relaxation time τ characteristic of the terminal zone corresponds to the rotational relaxation time of the elongated micelle. Application of the theory of Brownian motion of a rigid rod in the semidilute regime then permits us to estimate the apparent rod length L of the micelle using Eqs. (4–7) [63] where the end effect is ignored for simplicity.

Table 2. Applicability of the theory of Brownian motion of a rigid rod in the semidilute regime to dynamics of CTAB:NaSal micelles in aqueous solution

T/°C	C_s/C_D	L/nm	$\frac{D_{exp}}{D_{cal}}$	$\frac{\tau_{exp}}{\tau_{cal}}$	$\frac{J_{e,exp}}{J_{e,calc}}$
25	1	1870	0.18	5.5	–
25	2	1220	0.24	4.2	0.43
25	4	955	0.4	2.5	0.44
25	10	1130	0.34	2.9	0.21
25	20	890	0.13	7.8	0.68
25	41	600	0.20	4.9	1.05
33	1	1540	0.29	3.5	0.76
33	2	1030	0.32	3.1	0.49
33	4	810	0.84	1.2	0.50
33	10	1020	0.86	1.1	0.24
33	20	870	0.46	2.1	0.37
33	41	730	0.84	1.2	1.1
40	1	1100	0.24	4.1	0.89
40	2	910	0.39	2.6	0.61
40	4	810	1.04	0.95	0.52
40	10	860	1.2	0.85	0.32
40	20	820	0.85	1.2	0.39
40	41	880	1.67	0.59	3.6
50	1	700	0.21	4.7	1.32
50	2	750	0.54	1.8	0.63
50	4	845	2.1	0.47	0.75
50	10	835	2.0	0.49	1.3
50	20	930	1.9	0.52	1.4
50	41	1100	3.2	0.31	13.7

$$D_t = D_{t,0}/2 \tag{4}$$

$$\tau = 1/6D_r = (nL^3)^2/6\beta D_{r,0} \tag{5}$$

$$D_{t,0} = k_B T \ln(L/d)/3\pi\eta_s L \tag{6}$$

$$D_{r,0} = 3k_B T \ln(L/d)/\pi\eta_s L^3 \,. \tag{7}$$

Here, D obtained by FRS measurements is identified as the translational diffusion coefficient D_t of a rod, $D_{t,0}$ and $D_{r,0}$ are the translational and the rotational diffusion coefficient of the micelle with the same length L at infinite dilution, respectively, n and d the number density and the diameter of

the rod, and β the proportionality constant to be put as 1320 [64]. Following the simple procedure described in ref. [50], we can uniquely determine L from values of D and τ given in Table 1. Substituting values of L estimated into Eqs. (4) and (5), we may calculate D_{calc}, τ_{calc} and $J_{e,calc}$ ($\equiv n/k_BT$). In Table 2 we give ratios of D_{exp}/D_{calc}, τ_{exp}/τ_{calc}, and $J_{e,exp}/J_{e,calc}$ as a convenient check of agreement between theory and experiment. The agreement is poor at lower C_s/C_D but not bad at higher C_s/C_D. Thus, we suggest that the rigid rod model can be considered a successful one for semiquantitative but simultaneous description of the diffusion and viscoelastic behaviors of the CTAB: NaSal micelle system at low surfactant concentration of $C_D = 0.01$ M.

Acknowledgments

We are grateful to Prof. K. Osaki for valuable discussion. This work is partially supported by a Grant-in-Aid for Scientific Research (No. 03453113) of the Ministry of Culture, Science and Education of Japan.

References

1. Thurn H, Löbl M, Hoffmann H (1985) J Phys Chem 89:517
2. Rehage H, Hoffmann H (1988) J Phys Chem 92:4712; (1991) Mol Phys 74:933
3. Hoffmann H, Rauscher A, Gradzielski M, Schulz SF (1992) Langmuir 8:2140
4. Hoffmann H, Rehage H, Rauscher A (1992) In Chen SH et al. (eds) Structure and Dynamics of Strongly Interacting Colloids and Supramolecular Aggregates in Solution, Kluwer Academic Pub:Netherlands pp 493
5. Gamboa C, Sepúlveda L (1986) J Colloid Interface Sci 113:566
6. Shikata T, Hirata H, Kotaka T (1987) Langmuir 3:1081; (1988) Langmuir 4:354; (1989) Langmuir 5:398
7. Shikata T, Hirata H, Takatori E, Osaki K (1988) J Non-Newtonian Fluid Mech 28:171
8. Yamamura T, Kusaka T, Takatori E, Inoue T, Nemoto N, Osaki K, Shikata T, Kotaka T (1991) Nihon Reoroji Gakkaishi 19:45 (in Japanese)
9. Yamamura T, Nemoto N, Shikata T, Osaki K (1991) Nihon Reoroji Gakkaishi 19:140 (in Japanese)
10. Candau SJ, Hirsch E, Zana R, Delsantai M (1989) Langmuir 5:1225
11. Cates ME, Candau SJ (1990) J Phys Condens Matter 2:6869
12. Kern F, Zana R, Candau SJ (1991) Langmuir 7:1344
13. Kern F, Lemarechal P, Candau SJ, Cates ME (1992) Langmuir 8:437
14. Sasaki M, Imae T, Ikeda S (1989) Langmuir 5:211
15. Hashimoto K, Imae T, Nakazawa K (1992) Colloid Polym Sci 270:249
16. Clausen TM, Vinson PK, Minter JR, Davis HT, Talmon Y, Miller WG (1992) J Phys Chem 96:474
17. Cates ME (1987) Macromolecules 20:2289; (1990) J Phys Chem 94:371
18. Cates ME, Marques CM, Bouchard J-P (1991) J Chem Phys 94:8529
19. Drye TJ, Cates ME (1992) J Chem Phys 96:1367
20. Granek R, Cates ME (1992) J Chem Phys 96:4758
21. Turner MS, Cates ME (1992) J Phys II France 2:503
22. Mackintosh FC, Safran SA, Pincus PA (1990) Europhys Lett 12:697
23. Shikata T, Sakaiguchi Y, Urakami H, Tamura A, Hirata H (1987) J Colloid Interface Sci 119:291
24. Sakaiguchi Y, Shikata T, Urakami H, Tamura A, Hirata H (1987) Colloid Polym Sci 265:750
25. Wolff T, Emming C-S, von Bünau G, Zierold K (1992) Colloid Polym Sci 270:822
26. Ulmis J, Wennerström H, Johannson LB-A, Lindbolm G, Gravsholt S (1979) J Phys Chem 83:2232
27. Manohar C, Rao URK, Volaulikar BS, Iyer RM (1986) J Chem Soc Chem Commun 379
28. Anet FAL (1986) J Am Chem Soc 108:7102
29. Olsson U, Söderman O, Guering P (1986) J Phys Chem 90:5223
30. Rao URK, Manohar C, Volaulikar BS, Iyer RN (1987) J Phys Chem 91:3286
31. Quirion F, Magid LJ (1986) J Phys Chem 90:5435
32. Hayter JB, Penfold J (1983) Colloid Polym Sci 261:1022
33. Porte G, Appell J, Poggl Y (1980) J Phys Chem 84:3105
34. Candau SJ, Hirsch E, Zana R (1985) J Colloid Interface Sci 105:521
35. Candau SJ, Hirsch E, Zana R, Adan M (1988) J Colloid Interface Sci 122:430
36. Makhloufi R, Hirsch E, Candau SJ, Binana-Limbele W, Zana R (1989) J Phys Chem 93:8095
37. Candau SJ, Merikhi F, Waton G, Lemarachal P (1990) J Phys France 51:977
38. Appell J, Porte G (1990) Europhys Lett 12:185
39. Appell J, Porte G, Khatory A, Kern F, Candau SJ (1992) J Phys France II 2:1045
40. Imae T, Kamiya R, Ikeda S (1985) J Colloid Interface Sci 108:215
41. Imae T, Ikeda S (1986) J Phys Chem 90:5216
42. Imae T (1989) Colloid Polym Sci 267:707; (1990) J Phys Chem 94:5953
43. Brown W, Johansson K, Almgren M (1989) J Phys Chem 93:5888
44. Ng SC, Gan LM, Chew CH (1992) Colloid Polym Sci 270:64
45. Magid L (1993) In Brown W (eds), Dynamic Light Scattering, The Method and Some Applications, Clarendon Press: Oxford pp 554
46. Rehage H, Hoffmann H, Winderlich I (1986) Ber Bunsenges Phys Chem 90:1071
47. Hoffmann H, Kramer U, Thurn H (1990) J Phys Chem 94:2027
48. Wu X-I, Yeung C, Kim MW, Huang JS, Ou-Yang D (1992) Phys Rev Lett 68:1426
49. Messager R, Ott A, Chatenay D, Urbach W, Langevin D (1988) Phys Rev Lett 60:1410

50. Nemoto N, Yamamura T, Osaki K, Shikata T (1991) Langmuir 7:2607
51. Nemoto N, Kuwahara M (1993) Langmuir 9:419
52. Koike A, Yamamura T, Nemoto N (1994) Colloid Polym Sci 272:000
53. Inoue T, Nemoto N, Kojima T, Tsunashima Y, Kurata M (1986) Nihon Reoroji Gakkaishi 16:72 (in Japanese)
54. Inoue T, Nemoto N, Kojima T, Kurata M (1988) Polym J 20:869
55. Ott A, Bouchard JP, Langevin D, Urbach W (1990) Phys Rev Lett 65:2201
56. Ferry JD (1980) Viscoelastic Properties of Polymers, John Wiley & Sons Inc: New York
57. In preparation
58. Warren TC, Scharg JL, Ferry JD (1973) Biopolymers 12:1905
59. Nemoto N, Scharg JL, Ferry JD, Fullton RW (1975) Biopolymers 14:409
60. Nemoto N, Scharg JL, Ferry JD (1975) Polymer J 7:195
61. Rosser RW, Nemoto N, Scharg JL, Ferry JD (1978) Biopolymers 16:1031
62. Nemoto N (1979) Nihon Reoroji Gakkaishi 7:3 (in Japanese)
63. Doi M, Edwards SF (1986) The Theory of Polymer Dynamics, Oxford University Press: Oxford
64. Teraoka S, Oukubo N, Hayakawa R (1985) Phys Rev Lett 55:2712

Received May 24, 1993;
accepted September 22, 1993

Authors' address:

Prof. Dr. Norio Nemoto
Institute for Chemical Research
Kyoto University
Uji, Kyoto 611, Japan